Research Letter

Nanotube Boiler: Attogram Copper Evaporation Driven by Electric Current, Joule Heating, Charge, and Ionization

Lixin Dong, *Member, IEEE*, Xinyong Tao, Mustapha Hamdi, *Student Member, IEEE*, Li Zhang, Xiaobin Zhang, Antoine Ferreira, *Member, IEEE*, and Bradley J. Nelson, *Senior Member, IEEE*

***Abstract*—Controlled copper evaporation at attogram level from individual carbon nanotube (CNT) vessels, which we call nanotube boilers, is investigated experimentally and theoretically. We compared the evaporation modes induced by electric current, Joule heating, charge, and ionization in these CNT boilers, which can serve as sources for mass transport and deposition in nanofluidic systems. Experiments and molecular dynamics simulations show that the most effective method for evaporation is by positively ionizing the encapsulated copper; therefore, an electrostatic field can be used to guide the flow.**

***Index Terms*—Carbon nanotube, nanoboiler, nanofluidics, nanorobotic manipulation, transmission electron microscope.**

I. Introduction

CONTROLLED melting and flowing of mass within and between nanochannels is of great interest both fundamentally and from an application perspective [1]–[8]. We report an experimental and theoretical investigation into attogram copper evaporation from individual carbon nanotubes (CNTs), which is motivated by the need to understand the mechanism of this phenomenon. Copper has played a significant role in the history of civilization. In the semiconductor industry, copper is increasingly replacing aluminum because of its superior electrical conductivity. Growing interest in using it as electrodes and functional elements for the next generation of integrated circuits has been stimulated by the discovery of CNTs, nanowires, and other building blocks and enabled by bottom-up nanotechnologies such as self-assembly [9], robotic assembly [10], and welding [6], [11]. With the possibility of delivering attogram copper from conduits [6], [7], copper-filled CNTs [12] are an ideal combination for self-welding of self-assembled nanotubes [9] onto electrodes, among other potential nanofluidic applications [13]–[15].

Previous experimental investigations of controlled melting and flowing of single crystalline copper from individual CNTs [6], [7] have shown that very low current induces melting and drives the flow, which is much more efficient than irradiation-based techniques involving high-energy electron beams [16]–[19], focused-ion beams (FIB) [20], or lasers [14]. Furthermore, conservation of the material is facilitated by its encapsulation as opposed to conveying mass on the external surface of nanotubes [21]. Because both the rate and direction of mass transport depend on the external electrical drive, precise control and delivery of minute amounts of material is possible. However, due to the coupling of the electronic and thermal effects, the mechanisms have not been well understood.

Manuscript received February 15, 2009; revised May 16, 2009. First published June 30, 2009; current version published September 4, 2009. This work was supported by the Swiss Federal Institute of Technology (ETH-Zurich), by the Chinese National Science Foundation (50571087), by the Hi-tech Research and Development Program of China (863) (2002 AA334020), and by the Natural Sciences Fund of Zhejiang Province (Y404274). The review of this paper was arranged by Associate Editor J. Li.

L. Dong was with the Institute of Robotics and Intelligent Systems, the Swiss Federal Institute of Technology Zurich (ETH Zurich), 8092 Zurich, Switzerland. He is now with the Michigan State University, East Lansing, MI 48824-1226, USA (e-mail: ldong@ethz.ch).

X. Tao was with the Department of Materials Science and Engineering, Zhejiang University, Hangzhou 310027, China. He is now with the College of Chemical Engineering and Materials Science, Zhejiang University of Technology, Hangzhou 310032, China (e-mail: xinyongtao@gmail.com).

M. Hamdi and A. Ferreira are with the Institut Pluridisciplinaire de Recherche en Ingénierie des Systèmes, Mécanique et Energétique (PRISME), Ecole Nationale Supérieure d'Ingénieurs (ENSI), 18000 Bourges, France (e-mail: mfhamdi@gmail.com; antoine.ferreira@ensi-bourges.fr).

L. Zhang and B. J. Nelson are with the Institute of Robotics and Intelligent Systems, the Swiss Federal Institute of Technology Zurich (ETH Zurich), 8092 Zurich, Switzerland (e-mail: lizhang@ethz.ch; bnelson@ethz.ch).

X. Zhang is with the Department of Materials Science and Engineering, Zhejiang University, Hangzhou 310027, China (e-mail: zhangxb@zju.edu.cn).

Color versions of one or more of the figures in this paper are available online at http://ieeexplore.ieee.org.

Digital Object Identifier 10.1109/TNANO.2009.2026172

II. System Setup

To understand the mechanisms induced by various physical effects, experimental investigations have been done using the setup shown in Fig. 1, where two Cu-filled CNTs supported on a common sample holder and a probe provide four different experimental modes: 1) The upper section of the left nanotube $CNT_{1,A}$ has electric current passing through and accordingly Joule heating will occur. 2) The lower section of the left nanotube $CNT_{1,B}$ has no current and will experience only thermal transport. In (3) and (4), the right tube CNT_2 has no electric current but can be either negatively charged or positively ionized. Thermal transport also occurs from the common sample holder, but not as directly as $CNT_{1,B}$ due to CNTs superior heat conduction ability (thermal conductivity: 3320 W/m·K; c.f. Ag: 429 W/m·K, Cu: 386 W/m·K, Au: 318 W/m·K) [22].

The samples we use are Cu-filled CNTs. As described elsewhere, the Cu-tipped CNT samples are synthesized using an alkali-doped Cu catalyst by a thermal chemical vapor deposition (CVD) method [12]. The CNTs are up to 5 μm long with outer diameters in a range of 40–80 nm. The single crystalline Cu

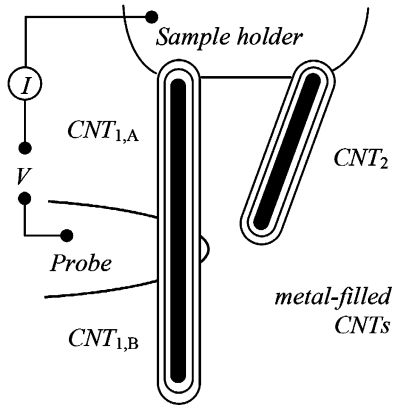

Fig. 1. Schematic setup of a nanotube boiler. Two Cu-filled CNTs supported on a sample holder and a probe provide three different cases to investigate, $\mathrm{CNT}_{1,\mathrm{A}}$, $\mathrm{CNT}_{1,\mathrm{B}}$, and CNT_2, subjected to electric current, thermal transport, and charges, respectively.

nanoneedles are encapsulated in graphite walls approximately 4 to 6 nm thick at the tips. The graphite layers are not parallel to the tube axis.

III. Experiments

Our experiments were performed in a Philips CM30 transmission electron microscope (TEM) equipped with a scanning tunneling microscope (STM) built in a TEM holder (Nanofactory Instruments AB, ST-1000) serving as a manipulator [2], [6], [23]. The material consisting of a CNT bundle is attached to a 0.35-mm-thick Au wire using silver paint, and the wire is held in the sample holder (Fig. 1). An etched 10-μm thick tungsten wire with a tip radius of approximately 100 nm (Picoprobe, T-4-10-1mm) is used as the probe. The probe can be positioned in a millimeter-scale workspace with subnanometer resolution with the STM unit actuated by a 3-DOF piezotube, making it possible to select a specific CNT and pick it up. Physical contact can be made between the probe and the tip of a nanotube or between two nanotubes. Applying a voltage between the probe and the sample holder establishes an electrical circuit through a CNT and injects thermal energy into the system via Joule heating. By increasing the applied voltage, the local temperature can be increased past the melting point of the material encapsulated in a tube. The process is recorded by TEM images, a multimeter, and a nA meter. The acceleration voltage used in all experiments was 300 kV, the spot size of the electron beam was 100 nm, and the beam current density is in the range of regular imaging, i.e., about $1-2\ \mathrm{A/cm^2}$. This ensures that the beam does not have obvious influence on the evaporation.

Fig. 2 includes a series of TEM images recording the evaporation of Cu driven by current and Joule heating inside two single CNTs when the probe is positively biased (7 V). Both of the CNTs have caps on their two ends. It can be seen that the length of the copper core inside the CNT on the left side (both $\mathrm{CNT}_{1,\mathrm{A}}$ and $\mathrm{CNT}_{1,\mathrm{B}}$) decreases continuously. Fig. 3 is a series of TEM images recording the transport of Cu inside two single CNTs when the probe is negatively biased (-3.5V). It can be seen that the length of the copper core inside the CNT on the left side ($\mathrm{CNT}_{1,\mathrm{B}}$) also decreases continuously. Because the copper core is not between the electrodes, the polarity of the electrodes does not matter, copper will transport toward one of them.

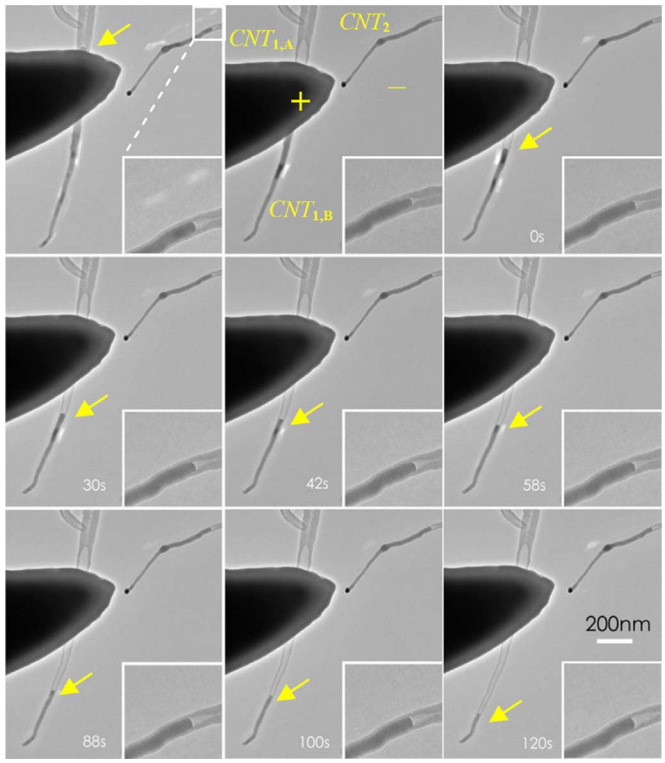

Fig. 2. Electric current and Joule heating driven Cu evaporation. A series of TEM images recorded the transport of Cu inside two single CNTs when the probe is positively biased (7 V). It can be seen that the length of the copper core inside the CNT on the left side continuously decreases.

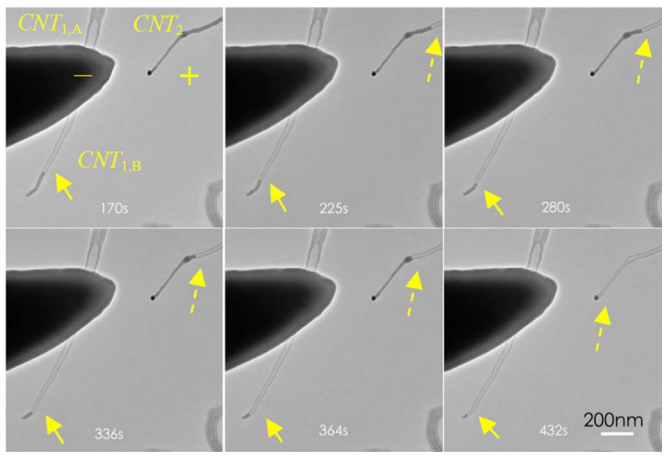

Fig. 3. Thermal transport and positive charges induced Cu evaporation. A series of TEM images recorded the transport of Cu inside two single CNTs when the probe is negatively biased (-3.5 V). It can be seen that the length of the copper core inside the CNT on the left side also continuously decreases.

Surprisingly, it can be seen from Fig. 3 that the length of the copper core inside the CNT on the right side (CNT_2) also decreases continuously until almost all copper disappears. A closer inspection of the insets of Fig. 2 reveals the same phenomena occurred when the probe is positively biased. This implies

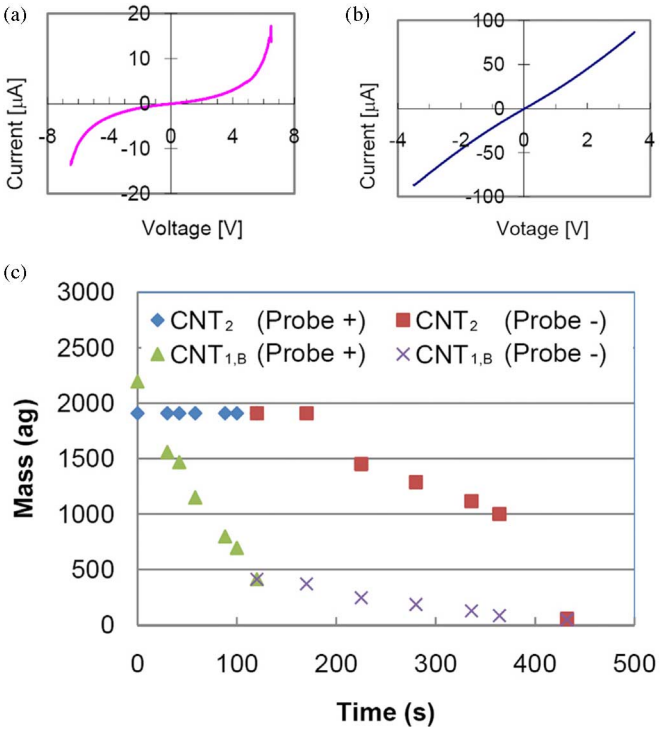

Fig. 4. (a) and (b) are I–V curves before the threshold on positive and negative biases is reached. It can be seen by comparing (a) and (b) that conductance improved after copper transport (the minimum resistance changed from (a) 377 to (b) 40 kΩ). (c) Mass evaporation rate.

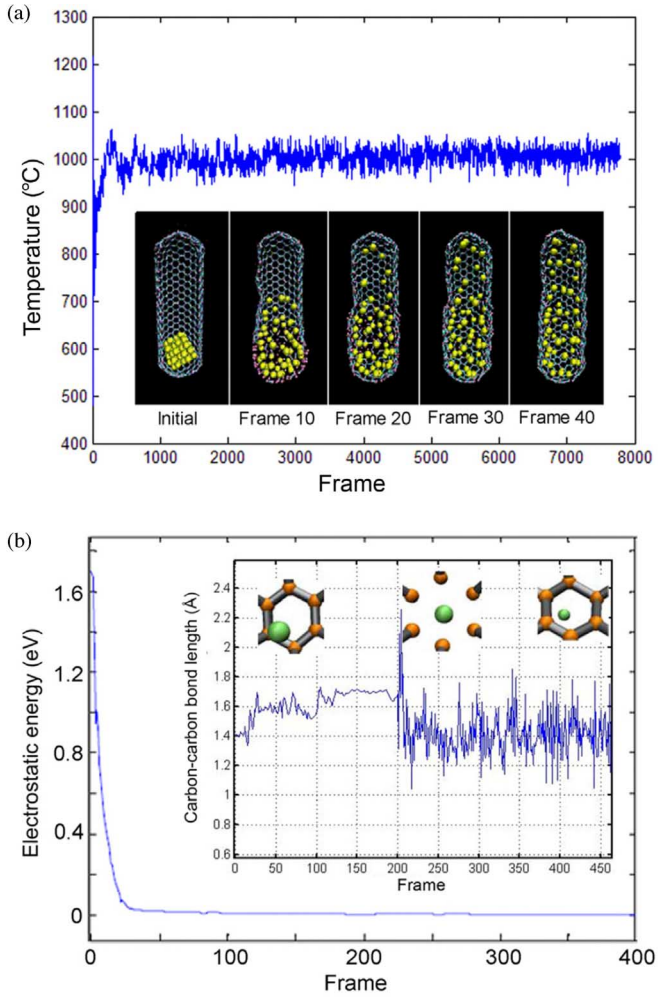

Fig. 5. Molecular dynamics simulation of Joule heating and ionization induced. (a) Evaporation induced by Joule heating. The diffusion of copper atoms inside the carbon shells can obviously be seen from the inset including the initial configuration and frames 10, 20, 30, and 40. (b) Electrostatic repulsive energy between copper ions. The inset shows carbon–carbon bond length during copper diffusion. At frame 200, the copper ions pass through the hexagonal rings, which correspond to the maximum opening of the carbon rings.

the possibility that charge-induced transport is more significant than current-induced Joule heating and thermal transport. The obvious difference of the evaporation rate for Cu inside CNT_2 suggests that as the Cu is positively ionized (Fig. 3), the repulsive forces between Cu ions are larger than negatively charged case (Fig. 2).

Fig. 4(a) and (b) are I–V curves before the positive and negative threshold biases are reached. It can be seen by comparing Fig. 4(a) and (b) that the conductance improved after the copper was transported (the minimum resistance changed from Fig. 4(a) 377 kΩ to Fig. 4(b) 40 kΩ). This suggests that the copper deposited on the probe in the case of Fig. 4(a) changed the contact from a Schottky-type to Ohmic. The decrease of resistance from 477 (−6.5) to 377 kΩ (6.5 V) in the case of Fig. 4(a) indicates the transport/deposition on the probe occurred during the bias sweeps from −6.5 to 6.5V.

Fig. 4(c) indicates the estimated mass evaporation rate according to the apparent geometries shown in Figs. 1 and 2 and the density of copper ($8.92\ \mathrm{g/cm^3}$). Using linear fitting, the average mass evaporation rate has been found to be 14.3 and 1.2 ag/s for $CNT_{1,B}$ as the probe is positively (Fig. 2) and negatively (Fig. 3) biased, respectively. The difference (approximately 12 times) between the rates of $CNT_{1,B}$ is due to the competition between electrostatic forces and Joule heating-induced evaporation. The latter is mainly caused by the different absolute values of the bias V (7 and −3.5 V) and the resistance R (377 to 40 kΩ). Considering that thermal power scales with V^2/R, the bias differences translate into a factor of 2.4, but the evaporation rate as the probe is negatively biased should be larger. This is contrary to the experimental observation. Hence, it can be concluded that electrostatic forces dominate evaporation. The growing distance from the heated section also has contribution but less due to the excellent thermal conductivity of CNTs.

Similarly, using linear fitting, the average mass evaporation rate has been found to be 0.1 and 6.1 ag/s for CNT_2 as the probe is positively (Fig. 2) and negatively biased (Fig. 3), respectively. This suggests that when Cu is ionized, the repulsive interaction between Cu^+ is much larger than electron charges.

IV. Simulations

Using molecular dynamics simulation (MDS), we numerically investigated pure Joule-heating and ionization-induced Cu evaporation (Fig. 5). The potential energy of a CNT with a cluster of Cu inside was minimized at an internal pressure of 1 atm using the conjugate gradient method. To investigate

copper diffusion, the system was simulated at temperatures between 700 and 1800 K using molecular dynamics. Fig. 5 (a) shows the system temperature during evaporation induced by Joule-heating when the carbon shells are electrically neutral. The diffusion of copper atoms inside the carbon shells can obviously be seen from the inset including the initial configuration and frames 10, 20, 30, and 40. An analysis of the repulsive electrostatic energy between copper ions is given in Fig. 5(b). It can be seen that a peak temperature was reached at frame 200. Accordingly, as shown in the inset, the carbon–carbon bond length obtained a maximum value at frame 200. The simulation indicates that electrostatic energy is responsible for heating, and that the repulsive charges increase the distances between copper ions and induce their diffusion with higher energy. It can be seen from the inset of Fig. 5(b) that with a large enough charge, copper ions can pass through the walls of CNTs without necessarily breaking the bonds. Images clearly show that the hexagon carbon rings stretch during diffusion.

V. Summary

In summary, we have reported an experimental and theoretical investigation into attogram copper evaporation from individual CNTs for four modes induced by electric current, Joule heating, charges, and ionization. The experimental setup allowed the decoupling of the modes from each other. Experiments and molecular dynamics simulations have shown that the most effective evaporation method is by positively ionizing the encapsulated copper, which indicates that the repulsive electrostatic energy between copper ions dominate thermal energy. The proposed CNT boilers can serve as sources for mass transport and deposition in nanofluidic systems using electrostatic fields to guide the flow.

Acknowledgment

The authors would like to thank the support from Electron Microscopy ETH Zurich (EMEZ).

References

[1] Y. H. Gao and Y. Bando, "Carbon nanothermometer containing gallium—Gallium's macroscopic properties are retained on a miniature scale in this nanodevice," *Nature*, vol. 415, pp. 599–599, Feb. 2002.

[2] K. Svensson, H. Olin, and E. Olsson, "Nanopipettes for metal transport," *Phys. Rev. Lett.*, vol. 93, no. 14, pp. 145901-1–145901-4, Oct. 2004.

[3] A. K. Schaper, F. Phillipp, and H. Q. Hou, "Melting behavior of copper nanocrystals encapsulated in onion-like carbon cages," *J. Mater. Res.*, vol. 20, pp. 1844–1850, Jul. 2005.

[4] L. Sun, F. Banhart, A. V. Krasheninnikov, J. A. Rodriguez-Manzo, M. Terrones, and P. M. Ajayan, "Carbon nanotubes as high-pressure cylinders and nanoextruders," *Science*, vol. 312, pp. 1199–1202, May 2006.

[5] M. Majumder, N. Chopra, R. Andrews, and B. J. Hinds, "Nanoscale hydrodynamics—Enhanced flow in carbon nanotubes," *Nature*, vol. 438, p. 44, Nov. 2005.

[6] L. X. Dong, X. Y. Tao, L. Zhang, X. B. Zhang, and B. J. Nelson, "Nanorobotic spot welding: Controlled metal deposition with attogram precision from copper-filled carbon nanotubes," *Nano Lett.*, vol. 7, pp. 58–63, Jan. 2007.

[7] D. Golberg, P. Costa, M. Mitome, S. Hampel, D. Haase, C. Mueller, A. Leonhardt, and Y. Bando, "Copper-filled carbon nanotubes: Rheostat-like Behavior and femtogram copper mass transport," *Adv. Mater.*, vol. 19, pp. 1937–1942, Aug. 2007.

[8] P. M. F. J. Costa, D. Golberg, M. Mitome, S. Hampel, A. Leonhardt, B. Buchner, and Y. Bando, "Stepwise current-driven release of attogram quantities of copper iodide encapsulated in carbon nanotubes," *Nano Lett.*, vol. 8, pp. 3120–3125, Oct. 2008.

[9] A. Subramanian, L. X. Dong, J. Tharian, U. Sennhauser, and B. J. Nelson, "Batch fabrication of carbon nanotube bearings," *Nanotechnology*, vol. 18, pp. 075703-1–075703-9, Feb. 2007.

[10] L. X. Dong, A. Subramanian, and B. J. Nelson, "Carbon nanotubes for nanorobotics," *Nano Today*, vol. 2, pp. 12–21, Dec. 2007.

[11] H. Hirayama, Y. Kawamoto, Y. Ohshima, and K. Takayanagi, "Nanospot welding of carbon nanotubes," *Appl. Phys. Lett.*, vol. 79, pp. 1169–1171, Aug. 2001.

[12] X. Y. Tao, X. B. Zhang, J. P. Cheng, Z. Q. Luo, S. M. Zhou, and F. Liu, "Thermal CVD synthesis of carbon nanotubes filled with single-crystalline Cu nanoneedles at tips," *Diamond Related Mater.*, vol. 15, pp. 1271–1275, Sep. 2006.

[13] S. Supple and N. Quirke, "Rapid imbibition of fluids in carbon nanotubes," *Phys. Rev. Lett.*, vol. 90, no. 21, pp. 214501-1–214501-4, May 2003.

[14] P. Kral and D. Tomanek, "Laser-driven atomic pump," *Phys. Rev. Lett.*, vol. 82, pp. 5373–5376, 1999.

[15] M. Whitby and N. Quirke, "Fluid flow in carbon nanotubes and nanopipes," *Nature Nanotechnol.*, vol. 2, pp. 87–94, Feb. 2007.

[16] L. X. Dong, F. Arai, and T. Fukuda, "Electron-beam-induced deposition with carbon nanotube emitters," *Appl. Phys. Lett.*, vol. 81, pp. 1919–1921, Sep. 2002.

[17] T. Yokota, M. Murayama, and J. M. Howe, "*In situ* transmission-electronmicroscopy investigation of melting in submicron Al-Si alloy particles under electron-beam irradiation," *Phys. Rev. Lett.*, vol. 91, no. 26, pp. 265504-1–265504-4, Dec. 2003.

[18] S. Y. Xu, M. L. Tian, J. G. Wang, H. Xu, J. M. Redwing, and M. H. W. Chan, "Nanometer-scale modification and welding of silicon and metallic nanowires with a high-intensity electron beam," *Small*, vol. 1, pp. 1221–1229, Dec. 2005.

[19] G. Q. Xie, M. H. Song, K. Furuya, D. V. Louzguine, and A. Inoue, "Compound nanostructures formed by metal nanoparticles dispersed on nanodendrites grown on insulator substrates," *Appl. Phys. Lett.*, vol. 88, pp. 263120-1–263120-3, Jun. 2006.

[20] R. Kometani, K. Kanda, Y. Haruyama, T. Kaito, and S. Matsui, "Evaluation of field electron emitter fabricated using focused-ion-beam chemical vapor deposition," *Jpn. J. Appl. Phys. Part 2-Lett. Exp. Lett.*, vol. 45, pp. L711–L713, Jul. 2006.

[21] B. C. Regan, S. Aloni, R. O. Ritchie, U. Dahmen, and A. Zettl, "Carbon nanotubes as nanoscale mass conveyors," *Nature*, vol. 428, pp. 924–927, Apr. 2004.

[22] P. G. Collins and P. Avouris, "Nanotubes for electronics," *Sci. Amer.*, vol. 283, pp. 62–69, Dec. 2000.

[23] L. X. Dong, K. Y. Shou, D. R. Frutiger, A. Subramanian, L. Zhang, B. J. Nelson, X. Y. Tao, and X. B. Zhang, "Engineering multiwalled carbon nanotubes inside a transmission electron microscope using nanorobotic manipulation," *IEEE Trans. Nanotechnol.*, vol. 7, no. 4, pp. 508–517, Jul. 2008.